Bit-Interleaved Coded Modulation With Mismatched Decoding Metrics

Trung Thanh Nguyen and Lutz Lampe
Department of Electrical and Computer Engineering
The University of British Columbia, Vancouver, Canada
Email: {trungn, lampe}@ece.ubc.ca

Abstract

Bit-interleaved coded modulation (BICM) has become the de facto coding standard for communication systems. Recently, BICM has been cast as a mismatched decoding scheme due to the assumption of independent bit metrics. In addition to this inherent mismatch, practical demodulators may produce mismatched decoding metrics because of implementation constraints, such as clipping and metric approximation to reduce computational complexity. In this paper, we investigate BICM with such metrics. In line with recent works on this topic, we adopt the generalized mutual information (GMI) as the pertinent performance measure. First, we show that level-dependent scaling of logarithmic bit metrics can improve the BICM GMI. Second, we propose a uniform metric scaling which can lead to an improved performance of mismatched sum-product symbol-by-symbol decoding, even if the GMI is not changed. Third, we investigate general metric-mismatch correction methods and analyze their effects in terms of the GMI. By means of three application examples, we illustrate that metric-mismatch correction, including metric scaling, can significantly increase BICM rates.

Index Terms

Bit-interleaved coded modulation (BICM), mismatched decoding, generalized mutual information (GMI), symbol-by-symbol decoding, metric correction.

I. Introduction

Bit-interleaved coded modulation (BICM) is a way of combining binary error-control codes with multilevel constellations. Invented in 1992 by Zehavi [1], it has become the de facto coding standard for modern communication systems thanks to its excellent performance and its flexibility in allowing separate code and modulation design. An up-to-date overview of BICM can be found in [2].

In a recent work by Martinez et al. [3], the BICM decoder has been cast as a mismatched decoder [4], [5] and the generalized mutual information (GMI) [4] has been used as a performance measure. This new perspective readily enables the study of BICM with mismatched demodulators, that is, when a twofold mismatch occurs. The first mismatch is due to the assumption of independent bit metrics and is inherent to BICM. The second mismatch occurs because of some approximation in the computation of bit metrics, such as quantization or clipping. Following this direction, Jaldén et al. [6] have recently devised and analyzed a metric correction method for BICM with mismatched demodulation.

In this paper we extend this new line of work. In particular, we study the manipulation of mismatched bit metrics to improve the performance of BICM. We start in Section II by first revisiting the concept of GMI and introducing the "I-curve," whose maximum is the GMI. We establish that the BICM I-curve is equal to the sum of the binary I-curves of the levels. This relation suggests that the GMI of BICM can be increased by aligning the binary I-curves so that their peaks are added in a totally constructive manner. In Section III-A, we show that this alignment can be achieved by scaling the log-likelihood ratio (LLR) metrics with suitable constant factors. In Section III-B, we investigate the effect of metric scaling on sum-product symbol-by-symbol (SBS) decoding, which is used in a number of state-of-the-art error-control coding systems, but for which the concept of GMI does not apply. Based on the properties of the I-curve, we propose a scaling rule which is demonstrated to lead to rate improvements in SBS decoding. Finally, in Section III-C, we consider the BICM demodulator as part of a cascaded channel. This point of view naturally leads to metric correction methods that increase the BICM GMI, including the scalar function used in [6], and new vector functions which provide different performance-complexity trade-offs. By three specific application examples in Section IV, we provide extensive numerical evidence that the proposed metric manipulations can improve the

performance of BICM. Concluding remarks are presented in Section V.

II. Mismatched Decoding: Random Coding Exponent, GMI, and BICM

We first briefly review the concept of the random coding exponent and the GMI, and their application to BICM from the mismatched decoding perspective. We then introduce the notion of I-curve and establish the relationship between the BICM I-curve and those of the BICM levels.

A. Random Coding With A Given Decoding Rule

Consider a discrete-time memoryless channel whose random input and output variable are denoted X and Y, respectively, and whose transition probability function is $p_{Y|X}(y|x)$. Input symbols are drawn from the discrete alphabet $\mathcal{X}$ with the probability mass function $p_X(x)$. The discrete or continuous output alphabet is denoted $\mathcal{Y}$. Given a received symbol $y \in \mathcal{Y}$, a symbol metric of the general form $q_{X,Y}(x,y)$ can be calculated for each $x \in \mathcal{X}$. We assume that $q_{X,Y}(x,y) > 0$, $\forall x \in \mathcal{X}$, $y \in \mathcal{Y}$. Consider a code with the codebook $\mathcal{C}$ that consists of K length-N codewords $\boldsymbol{x} = [x_0 \dots x_{N-1}]$. Each codeword in $\mathcal{C}$ is equally likely chosen for transmission. Given the received sequence $\boldsymbol{y} = [y_0 \dots y_{N-1}]$, for each $\boldsymbol{x} \in \mathcal{C}$, the word metric is calculated as

$$q_{\boldsymbol{X},\boldsymbol{Y}}(\boldsymbol{x},\boldsymbol{y}) = \prod_{k=0}^{N-1} q_{X,Y}(x_k, y_k) \ . \tag{1}$$

The decoder output is determined by

$$\hat{\boldsymbol{x}} = \underset{\boldsymbol{x}\in\mathcal{C}}{\operatorname{argmax}} \ q_{\boldsymbol{X},\boldsymbol{Y}}(\boldsymbol{x},\boldsymbol{y}) \ . \tag{2}$$

The symbol metric $q_{X,Y}(x,y)$ is called a matched metric if it is proportional to the channel transition probability $p_{Y|X}(y|x)$. It is called a mismatched metric otherwise [4], [5]. With matched metrics, (2) coincides with the maximum-likelihood (ML) decoding rule and, since all codewords are equally likely, it minimizes the word error probability [7, p. 120].

The word error probability, averaged over all codewords and random codebook realizations, can be upper-bounded by [7, Ch. 5], [4, Sec. 2], [2, Sec. 3.1.2]

$$P_{\mathrm{w}} \leq 2^{-NE^{\mathrm{r}}_{q_{X,Y}}(R)}, \tag{3}$$

where R is any positive number such that $K - 1 < 2^{NR} \leq K$,

$$E^{\mathrm{r}}_{q_{X,Y}}(R) \triangleq \max_{0\leq\rho\leq 1} \max_{s>0} \left(E^0_{q_{X,Y}}(\rho, s) - \rho R \right) \tag{4}$$

is the random coding exponent, and

$$E_{q_{X,Y}}^{0}(\rho,s) \triangleq -\log \mathcal{E}_{X,Y}\left\{\left(\sum_{x\in\mathcal{X}} p_X(x)\left[\frac{q_{X,Y}(x,Y)}{q_{X,Y}(X,Y)}\right]^s\right)^{\rho}\right\} \tag{5}$$

is the generalized Gallager function ($\log(\cdot)$ denotes logarithm with base 2). If $E_{q_{X,Y}}^{\mathrm{r}}(R) > 0$, the error probability vanishes with increasing N and the rate R is said to be achievable. The maximum achievable rate that can be inferred from (4) and the properties of $E_{q_{X,Y}}^{0}(\rho,s)$, cf. [7, Theorem 5.6.3], is the GMI, which is defined as [4]

$$I_{q_{X,Y}}^{\mathrm{gmi}} \triangleq \max_{s>0} I_{q_{X,Y}}(s)\ , \tag{6}$$

with

$$I_{q_{X,Y}}(s) \triangleq \left.\frac{\partial E_{q_{X,Y}}^{0}(\rho,s)}{\partial\rho}\right|_{\rho=0} = \lim_{\rho\to 0}\frac{E_{q_{X,Y}}^{0}(\rho,s)}{\rho} = -\mathcal{E}_{X,Y}\left\{\log\sum_{x\in\mathcal{X}} p_X(x)\left[\frac{q_{X,Y}(x,Y)}{q_{X,Y}(X,Y)}\right]^s\right\}\ . \tag{7}$$

We call the plot of $I_{q_{X,Y}}(s)$ vs. s the I-curve of the metric $q_{X,Y}(x,y)$. The peak value of the I-curve is the GMI.

B. BICM and Mismatched Decoding

We now focus on the BICM scheme [2]. At the transmitter, a binary encoder is connected to a multilevel modulator, and at the receiver, a demodulator produces decoding metrics for the binary decoder. We note that, despite the "bit-interleaved" part in the name of BICM, bit interleaving is immaterial for the random coding argument [3] and also not needed in many practical situations[1]. Therefore, we do not include such bit (de)interleavers in our discussion.

Let 2^m be the size of the constellation $\mathcal{X}$ and $B_0,\ldots,B_{m-1}$ be the m binary random variables for the labeling bits of the transmit symbol. Furthermore, let $b_i(x)$ be the i-th bit in the label of symbol x. The probability mass functions $p_{B_i}(b)$, $b\in\mathcal{B}\triangleq\{0,1\}$, and $p_X(x)$, $x\in\mathcal{X}$, are related by

$$p_{B_i}(b) = \sum_{x\in\mathcal{X}_i^b} p_X(x)\ , \tag{8}$$

[1]When using low-density parity check (LDPC) codes, for example, bit-interleaving is equivalent to re-ordering the columns of the parity-check matrix, which does not affect decoding outcome.

where $\mathcal{X}_i^b \triangleq \{x \in \mathcal{X} : b_i(x) = b\}$, and

$$p_X(x) = \prod_{i=0}^{m-1} p_{B_i}(b_i(x)) \ . \tag{9}$$

Instead of directly producing 2^m symbol-metric values for each possible x given the received symbol y, the BICM demodulator produces $2m$ bit-metric values corresponding to the m levels. Bit metrics for the i-th level have the general form $q_{B_i,Y}(b,y)$. We also assume $q_{B_i,Y}(b,y) > 0$, $\forall b \in \mathcal{B}$, $\forall y \in \mathcal{Y}$. The symbol metric is then calculated as

$$q_{X,Y}(x,y) = \prod_{i=0}^{m-1} q_{B_i,Y}(b_i(x),y) \ . \tag{10}$$

Even if $q_{B_i,Y}(b,y)$ matches to the binary-input channel with input B_i and output Y, i.e., it is proportional to the transition probability

$$p_{Y|B_i}(y|b) = \sum_{x \in \mathcal{X}_i^b} p_{Y|X}(y|x) p_X(x) \ , \tag{11}$$

the symbol metric (10) still does not match to the channel with input X and output Y. Therefore, BICM is inherently a mismatched decoding scheme [2], [3].

1) Log-Likelihood Ratio (LLR): The binary decoder is fed with the $2m$ bit-metric values per received symbol, or alternatively, with m log-metric ratios

$$\Lambda_{q_{B_i,Y}}(y) \triangleq \ln \frac{q_{B_i,Y}(0,y)}{q_{B_i,Y}(1,y)} \ , \tag{12}$$

since they are sufficient statistics for B_i given $q_{B_i,Y}(b,y)$ ($\ln(\cdot)$ denotes the natural logarithm). Conventionally, $\Lambda_{q_{B_i,Y}}(y)$ is the LLR only if $q_{B_i,Y}(b,y) \propto p_{Y|B_i}(y|b)$. However, for convenience and brevity, we will refer to $\Lambda_{q_{B_i,Y}}(y)$ as an LLR even when $q_{B_i,Y}(b,y)$ is not proportional to $p_{Y|B_i}(y|b)$.

2) Independent Binary Channel Model: The classical approach to analyze BICM is to use the independent binary channel model [8], in which transmission is performed in m parallel channels with inputs B_i, $i = 0, \ldots, m-1$, and output Y. This model is equivalent to multilevel coding (MLC) with parallel decoding of levels [9]. For level i and its bit metric, the binary generalized Gallager function is defined as

$$E_{0,q_{B_i,Y}}(\rho,s) \triangleq -\log \mathcal{E}_{B_i,Y}\left\{\left(\sum_{b\in\mathcal{B}} p_{B_i}(b)\left[\frac{q_{B_i,Y}(b,Y)}{q_{B_i,Y}(B_i,Y)}\right]^s\right)^\rho\right\} \tag{13}$$

$$= -\log \mathcal{E}_{X,Y}\left\{\left(\sum_{b\in\mathcal{B}} p_{B_i}(b)\left[\frac{q_{B_i,Y}(b,Y)}{q_{B_i,Y}(b_i(X),Y)}\right]^s\right)^\rho\right\} \ , \tag{14}$$

where the transition from $\mathcal{E}_{B_i,Y}\{\cdot\}$ to $\mathcal{E}_{X,Y}\{\cdot\}$ is possible because the term inside the expectation in (14) is the same for all transmit symbols x that have the same i-th labeling bit, and

$$\sum_{x\in\mathcal{X}_i^b} p_{X,Y}(x,y) = p_{B_i,Y}(b,y)\ . \tag{15}$$

The function $E_{0,q_{B_i,Y}}(\rho,s)$ gives rise to the random coding exponent $E_{\mathrm{r},q_{B_i,Y}}(R)$, the I-curve function $I_{q_{B_i,Y}}(s)$, and the GMI $I^{\mathrm{gmi}}_{q_{B_i,Y}}$ for the i-th level, applying (4), (7), and (6), respectively. In particular,

$$\begin{aligned} I_{q_{B_i,Y}}(s) &= -\mathcal{E}_{B_i,Y}\left\{\log\sum_{b\in\mathcal{B}} p_{B_i}(b)\left[\frac{q_{B_i,Y}(b,Y)}{q_{B_i,Y}(B_i,Y)}\right]^s\right\} \\ &= -\mathcal{E}_{X,Y}\left\{\log\sum_{b\in\mathcal{B}} p_{B_i}(b)\left[\frac{q_{B_i,Y}(b,Y)}{q_{B_i,Y}(b_i(X),Y)}\right]^s\right\}\ , \end{aligned} \tag{16}$$

and

$$I^{\mathrm{gmi}}_{q_{B_i,Y}} = \max_{s>0} I_{q_{B_i,Y}}(s)\ . \tag{17}$$

For the special case of uniform input, from (12) and (16), $I_{q_{B_i,Y}}(s)$ can be expressed in terms of the LLR as

$$I_{q_{B_i,Y}}(s) = 1 - \mathcal{E}_{X,Y}\left\{\log(1+\exp(-\operatorname{sgn}(b_i(X))\Lambda_{q_{B_i,Y}}(Y)s)\right\}\ , \tag{18}$$

where the function $\operatorname{sgn}(\cdot)$ is defined for the labeling bits as $\operatorname{sgn}(0)=1$ and $\operatorname{sgn}(1)=-1$.

3) BICM and Binary I-curves: Substituting (9) and (10) into (7) and considering (16), we obtain (cf. [3, proof of Theorem 2])

$$\begin{aligned} I_{q_{X,Y}}(s) &= -\mathcal{E}_{X,Y}\left\{\log\sum_{x\in\mathcal{X}}\prod_{i=0}^{m-1} p_{B_i}(b_i(x))\left[\frac{q_{B_i,Y}(b_i(x),Y)}{q_{B_i,Y}(b_i(X),Y)}\right]^s\right\} \\ &= -\mathcal{E}_{X,Y}\left\{\log\prod_{i=0}^{m-1}\sum_{b\in\mathcal{B}} p_{B_i}(b)\left[\frac{q_{B_i,Y}(b,Y)}{q_{B_i,Y}(b_i(X),Y)}\right]^s\right\} \\ &= -\sum_{i=0}^{m-1}\mathcal{E}_{X,Y}\left\{\log\sum_{b\in\mathcal{B}} p_{B_i}(b)\left[\frac{q_{B_i,Y}(b,Y)}{q_{B_i,Y}(b_i(X),Y)}\right]^s\right\} \\ &= \sum_{i=0}^{m-1} I_{q_{B_i,Y}}(s)\ . \end{aligned} \tag{19}$$

That is, the BICM I-curve equals to the sum of the binary I-curves $I_{q_{B_i,Y}}(s)$. This relation will be important for our subsequent discussion.

III. Metric Manipulation

We now present and discuss different metric manipulations that can improve the performance of BICM with a mismatched demodulator.

A. Achievable Rate with Metric Scaling

For the general mismatched decoding scheme from Section II-A, let $s_{q_{X,Y}}$ be the critical point of $I_{q_{X,Y}}(s)$, i.e. the value of s at which $I_{q_{X,Y}}(s)$ attains its maximum. For matched metrics, $s_{q_{X,Y}} = 1$, and $I^{\text{gmi}}_{q_{X,Y}}$ equals to the ordinary mutual information $I(X;Y)$ [7]. Let us consider a new metric $q'_{X,Y}(x,y) = [q_{X,Y}(x,y)]^c$ with some constant $c > 0$. It follows from (5) that $E^0_{q'_{X,Y}}(\rho, s) = E^0_{q_{X,Y}}(\rho, cs)$ and hence $I_{q'_{X,Y}}(s) = I_{q_{X,Y}}(cs)$. That is, the I-curve of the metric $q'_{X,Y}(x,y)$ is simply a compressed (for $c > 1$) or expanded (for $c < 1$) version of the I-curve of the metric $q_{X,Y}(x,y)$ along the s-axis. In particular, the GMI remains unchanged, while the critical point changes to $s_{q'_{X,Y}} = s_{q_{X,Y}}/c$. This coordinate shift is illustrated in Figure 1 for an example with $c > 1$. Since raising $q_{X,Y}(x,y)$ to a power corresponds to scaling with the same factor in the logarithmic domain, in LLR-based decoding we refer to this operation as "metric scaling." Metric scaling allows us to control the critical point of the I-curve. The fact that it does not affect the GMI should not come as a surprise. Using $q'_{X,Y}(x,y)$, the decoding rule (2) becomes

$$\hat{\boldsymbol{x}} = \underset{\boldsymbol{x}\in\mathcal{C}}{\operatorname{argmax}} \ [q_{\boldsymbol{X},\boldsymbol{Y}}(\boldsymbol{x},\boldsymbol{y})]^c \ ,$$

which returns exactly the same codeword as using $q_{X,Y}(x,y)$. We now apply metric scaling to BICM.

Theorem 1: Let $s_{q_{B_i,Y}}$ be the critical point of the binary I-curve of the i-th level. Furthermore, let two I-curves be called harmonic if they have the same critical point. Then, the BICM GMI equals to the sum of the binary GMIs if the binary I-curves are harmonic, and less than that otherwise. The binary I-curves can be made harmonic at $s^* > 0$ by metric scaling with the factor $c_i = s_{q_{B_i,Y}}/s^*$ at level i, $i = 0, \ldots, m-1$.

Proof: Let $q'_{B_i,Y}(b,y) = [q_{B_i,Y}(b,y)]^{c_i}$ with some $c_i > 0$. Then, $I_{q'_{B_i,Y}}(s) = I_{q_{B_i,Y}}(c_i s)$, which peaks at $(s_{q_{B_i,Y}}/c_i, I^{\text{gmi}}_{q_{B_i,Y}})$. According to Section II-B and in particular (10) and (19), BICM with these bit metrics has $q'_{X,Y}(x,y) = \prod_{i=0}^{m-1} q'_{B_i,Y}(b_i(x),y)$ and $I_{q'_{X,Y}}(s) = \sum_{i=0}^{m-1} I_{q'_{B_i,Y}}(s)$. The

BICM GMI is upper-bounded as

$$I^{\text{gmi}}_{q'_{X,Y}} = \max_{s>0} \sum_{i=0}^{m-1} I_{q'_{B_i,Y}}(s) \leq \sum_{i=0}^{m-1} \max_{s>0} I_{q'_{B_i,Y}}(s) = \sum_{i=0}^{m-1} I^{\text{gmi}}_{q_{B_i,Y}} \ . \tag{20}$$

Equality in (20) is achieved if and only if all $I_{q'_{B_i,Y}}(s)$, $i = 0, \ldots, m-1$, attain their maximum at the same value of s, i.e. if they are harmonic. By scaling with $c_i = s_{q_{B_i,Y}}/s^*$, all binary I-curves will be harmonic at s^* for arbitrary $s^* > 0$. ■

Remark 1: If the original binary I-curves are already harmonic, no alignment is needed and $I^{\text{gmi}}_{q_{X,Y}} = \sum_{i=0}^{m-1} I^{\text{gmi}}_{q_{B_i,Y}}$. This is the case if, for example, $q_{B_i,Y}(b,y) \propto p_{Y|B_i}(y|b)$, for which $s_{q_{B_i,Y}} = 1 \ \forall i$ [3, Corollary 1]. When the binary I-curves are not harmonic (see Section IV for practical examples), the above proof provides a constructive procedure for choosing the scaling factors to increase the BICM GMI. This requires the computation of $s_{q_{B_i,Y}}$, $i = 0, \ldots, m-1$, which can be done offline, either through analysis or through simulation when closed-form expressions cannot be obtained.

Remark 2: According to the independent binary channel model, BICM always achieves a rate equal to the sum of the achievable rates of the levels. In the context of random coding and the GMI, Theorem 1 shows that this is only conditionally true. We recall that the independent binary channel model requires m binary encoder-decoder pairs instead of just one as BICM.

B. Symbol-By-Symbol Decoding and Metric Scaling

We again consider the general mismatched decoding scheme in Section II-A. The derivation of the random coding exponent and the GMI is based on the word decoding rule (2). However, some important modern error-correction schemes employ SBS decoding. That is, given the received sequence $\boldsymbol{y}$, for each position $k = 0, \ldots, N-1$, the SBS metric

$$q_{X_k,\boldsymbol{Y}}(x,\boldsymbol{y}) \triangleq \sum_{\boldsymbol{x} \in \mathcal{C}_k^x} q_{\boldsymbol{X},\boldsymbol{Y}}(\boldsymbol{x},\boldsymbol{y}) = \sum_{\boldsymbol{x} \in \mathcal{C}_k^x} \left(\prod_{k=0}^{N-1} q_{X,Y}(x_k, y_k) \right) \tag{21}$$

is computed, where $\mathcal{C}_k^x$ denotes the set of codewords whose k-th symbol equals x, and the decoding rule

$$\hat{x}_k = \operatorname*{argmax}_{x \in \mathcal{X}} \ q_{X_k,\boldsymbol{Y}}(x,\boldsymbol{y}) \tag{22}$$

is applied. For sparse-graph based codes, (22) with metric (21) can be efficiently evaluated (or approximated) using the sum-product algorithm [10]. With matched metrics and equally likely

chosen codewords, (22) becomes

$$\begin{aligned}\hat{x}_k &= \underset{x\in\mathcal{X}}{\operatorname{argmax}} \sum_{\boldsymbol{x}\in\mathcal{C}_k^x} p_{\boldsymbol{Y}|\boldsymbol{X}}(\boldsymbol{y}|\boldsymbol{x}) = \underset{x\in\mathcal{X}}{\operatorname{argmax}} \sum_{\boldsymbol{x}\in\mathcal{C}_k^x} p_{\boldsymbol{X}|\boldsymbol{Y}}(\boldsymbol{x}|\boldsymbol{y}) = \underset{x\in\mathcal{X}}{\operatorname{argmax}}\, p_{X_k|\boldsymbol{Y}}(x|\boldsymbol{y}) \\ &= \underset{x\in\mathcal{X}}{\operatorname{argmin}} \left(1 - p_{X_k|\boldsymbol{Y}}(x|\boldsymbol{y})\right) \ .\end{aligned}$$

Thus, sum-product SBS decoding with matched metrics minimizes the coded symbol error probability, cf. word decoding as in [7, p. 120]. This holds true regardless of the distribution $p_X(x)$. However, minimizing the coded symbol error probability may not be the same as minimizing the message symbol (or bit) or the word error probability. In particular, the collection of decoded symbols $[\hat{x}_0 \dots \hat{x}_{N-1}]$ is not necessarily a codeword in $\mathcal{C}$. Therefore, achievable rates, in the sense that the word error probability can still be driven to zero with increasing code length, further depend on the translation of the decoded symbols into a valid codeword.

Another popular SBS decoding metric is

$$q_{X_k,\boldsymbol{Y}}(x,\boldsymbol{y}) = \begin{cases} \max\limits_{\boldsymbol{x}\in\mathcal{C}_k^x} q_{\boldsymbol{X},\boldsymbol{Y}}(\boldsymbol{x},\boldsymbol{y}) = \max\limits_{\boldsymbol{x}\in\mathcal{C}_k^x} \left(\prod\limits_{k=0}^{N-1} q_{X,Y}(x_k,y_k) \right) \ , & \text{if } \mathcal{C}_k^x \neq \emptyset \\ 0 \ , & \text{otherwise .} \end{cases} \tag{23}$$

This metric can be estimated by the max-product algorithm, which is also known as the min-sum algorithm from its form in the logarithmic domain [10]. The metric (23) is derived from (21) by approximating a sum by its largest term.

As in word decoding, metric scaling does not affect the decoding outcome in max-product SBS decoding. However, if we replace $q_{X,Y}(x,y)$ by $[q_{X,Y}(x,y)]^c$ in sum-product decoding using (22), the decoding outcome might change. When $c \to 0$, the decoding outcome generally becomes random, with exceptions, e.g., repetition codes where the sum (21) would consist of only a single term. On the other hand, when $c \to \infty$, sum-product decoding approaches max-product decoding. With matched metrics, $c = 1$ is the optimal scaling factor when the coded symbol error probability is the performance measure. The I-curve peaks at $s = 1$ in this case. For mismatched metrics, we propose that metric scaling with the factor $c = s_{q_{X,Y}}$ is applied in sum-product decoding. This scaling shifts the critical point of the I-curve to 1. In the following, we provide a numerical example which shows that this scaling yields the largest throughput in a rateless transmission. (Further, practical examples that demonstrate performance improvements due to using this scaling are presented in Section IV.)

Example 1: Consider the binary asymmetric channel (BAC) with crossover probabilities p_0 and p_1, $0 < p_0, p_1 < 1$, for transmit symbol $x = 0$ and $x = 1$, respectively. A matched demodulator produces the LLR of $\ln((1-p_0)/p_1)$ for received symbol $y = 0$ and of $\ln(p_0/(1-p_1))$ for $y = 1$. Assuming uniform input, the matched I-curve follows from (7) or (18) as

$$I_{p_{Y|X}}(s) = 1 - \frac{1-p_0}{2}\log\left(1+\frac{p_1^s}{(1-p_0)^s}\right) - \frac{p_0}{2}\log\left(1+\frac{(1-p_1)^s}{p_0^s}\right) \\ -\frac{p_1}{2}\log\left(1+\frac{(1-p_0)^s}{p_1^s}\right) - \frac{1-p_1}{2}\log\left(1+\frac{p_0^s}{(1-p_1)^s}\right) , \quad (24)$$

which peaks at $(1, I(X;Y))$.

Suppose that a mismatched demodulator produces LLR of $+1$ and -1 for received symbol $y = 0$ and $y = 1$, respectively. The corresponding mismatched I-curve is given by

$$I_{q_{X,Y}}(s) = 1 - p\log(1+\mathrm{e}^s) - (1-p)\log(1+\mathrm{e}^{-s}) , \quad (25)$$

where $p = (p_0+p_1)/2$. The GMI $I^{\mathrm{gmi}}_{q_{X,Y}} = 1+p\log(p)+(1-p)\log(1-p) = 1-H_b(p)$ is attained at $s_{q_{X,Y}} = \ln((1-p)/p)$, where H_b is the binary entropy function. We have $I^{\mathrm{gmi}}_{q_{X,Y}} \le I(X;Y)$, and equality holds if and only if $p_0 = p_1$, i.e. when the channel is a binary symmetric channel (BSC). Applying scaling with factor c to this mismatched LLR, we obtain $I_{q'_{X,Y}}(s) = I_{q_{X,Y}}(cs)$. Consider $I_{q'_{X,Y}}(1)$ as a function of c. It attains its maximum with $c = s_{q_{X,Y}} = \ln((1-p)/p)$, for which $I_{q'_{X,Y}}(1) = I^{\mathrm{gmi}}_{q'_{X,Y}} = I^{\mathrm{gmi}}_{q_{X,Y}}$. Our proposal states that scaling with this value of c should be applied in sum-product decoding.

Let us consider a specific example with $p_0 = 0.03$ and $p_1 = 0.07$. This pair results in $I(X;Y) = 0.72$ bit per channel use (bpcu), $p = 0.05$, $I^{\mathrm{gmi}}_{q_{X,Y}} = 0.71$ bpcu, and $s_{q_{X,Y}} = 2.94$. Figure 2 shows the plot of $I_{q'_{X,Y}}(1)$ vs. c. To demonstrate the effect of scaling, we measure the average throughput achieved by coded transmission using a Raptor code. The code consists of an outer LDPC code of length $10\ 000$ and code rate 0.95 and an inner Luby transform (LT) code with degree distribution [11, Table I, second column]

$$\Omega(x) = 0.007969x + 0.493570x^2 + 0.166220x^3 + 0.072646x^4 + 0.082558x^5 \\ +0.056058x^8 + 0.037229x^9 + 0.055590x^{19} + 0.025023x^{65} + 0.003135x^{66} .$$

The parity-check matrix of the LDPC code is generated by the progressive edge growth (PEG) algorithm [12] with degree-3 variable nodes and almost regular check nodes. The transmitter sends coded bits until the receiver successfully determines the correct message, at which point

the instantaneous throughput is measured. Figure 2 shows the empirical average throughput achieved with sum-product and max-product decoding as a function of c (consider only lines labeled "w/o i.i.d. channel adapter" for the moment). Both methods use a maximum of 200 iterations to decode the joint factor graph of LDPC and LT code. We observe that scaling with the factor $c = s_{q_{X,Y}}$ indeed yields the best throughput for sum-product decoding. It can also be seen how the achieved throughput degrades as $c \to 0$. For large c, sum-product decoding starts to converge towards max-product decoding. However, since we applied LLR bounding for improved numerical stability in our decoder implementation, this convergence is not fully achieved in Figure 2.

We can turn the asymmetric channel into a symmetric one by using i.i.d. channel adapters suggested in [13]. These adapters are synchronized random sign-adjusters applied to the encoded bits and LLR streams at the transmitter and receiver, respectively, cf. [13, Fig. 8]. With uniform input, the I-curve is not changed by i.i.d. channel adaptation, cf. (18). Symmetrization is sometimes considered useful when codes are designed under the assumption of a symmetric channel. The simulation results for the symmetrized channel in Figure 2 (star makers labeled "w/ i.i.d. channel adapter") show that the conclusions about scaling are not an artifact of transmission over asymmetric channels.

Remark: Understanding the impact of metric scaling in fact relates to a familiar research problem. In systems with additive Gaussian noise, for example, inaccurate estimation of the signal-to-noise ratio (SNR) results in a mismatched metric that is a scaled version (in the logarithmic domain) of the matched metric. The scaling factor c is proportional to the estimated SNR. Thus, impact of SNR mismatch on sum-product decoding is a special case of our discussion. The results in Figure 2 agree with the known result that for sum-product decoding we would rather overestimate (have a large c) than underestimate the SNR (have a small c), cf. e.g. [14] and references therein. When $s_{q_{X,Y}} > 1$, which is the case of underestimated SNR, the simulation results in Figure 2 suggests an intriguing upper bound $I_{q_{X,Y}}(1)$ to the achievable rate with sum-product decoding.

We would like to contrast our scaling from LLR scaling as investigated in e.g. [15]–[17]. In these works, scaling is derived from studying the internal operation of the decoder and has the purpose of offsetting approximations to lower implementation complexity. On the other hand, our proposed scaling is characterized only by the metric and is aimed to improve the performance

of exact sum-product decoding.

Application to BICM: In connection with Theorem 1, in BICM with sum-product decoding we propose aligning all binary I-curves at $s^* = 1$. For max-product decoding, only the alignment matters, but not the value of the critical point s^*.

C. Cascaded Channel Perspective and Metric-Mismatch Correction

BICM as defined by (10), (1) and (2) constitutes a mismatched decoding rule, for which an achievable rate is given by the GMI $I^{\mathrm{gmi}}_{q_{X,Y}}$ defined in (6). In Section III-A, we have shown that metric scaling applied to LLRs $\Lambda_{q_{B_i,Y}}(y)$ can increase this GMI. In this section, we consider the generation of $\Lambda_{q_{B_i,Y}}(y)$ as part of the transmission channel and determine the rates achievable by further processing and other ways of decoding.

1) Cascaded Channel Model: Let $z_i \triangleq \Lambda_{q_{B_i,Y}}(y)$ be the channel output to be processed. Accordingly, we have a cascaded channel as shown in Figure 3(a) with input X and output $Z \triangleq [Z_0, \ldots, Z_{m-1}]$. The corresponding average mutual information $I(X;Z)$ is less than or equal to $I(X;Y)$ [7, Sec. 2.3]. Let us consider the use of binary codes for the cascaded channel $X \to Z$. The chain rule of mutual information [7, p. 22] reads as

$$I(X;Z) = \sum_{i=0}^{m-1} I(B_i; Z|B_0, \ldots, B_{i-1}) \; . \tag{26}$$

For the terms on the right-hand side, we have the following inequalities

$$\begin{aligned} I(B_i; Z|B_0, \ldots, B_{i-1}) &\geq I(B_i; Z) && (27)\\ &\geq I(B_i; Z_i) && (28)\\ &\geq I^{\mathrm{gmi}}_{q_{B_i,Y}} \; . && (29) \end{aligned}$$

The mutual information $I(B_i;Z)$ in (27) represents the constrained channel capacity, i.e. the maximum achievable rate with a given input distribution, of the binary-input channel $B_i \to Z$ illustrated in Figure 3(b). For this cascaded channel, $I(B_i;Z) \leq I(B_i;Y)$ [7, Sec. 2.3]. We note, however, that there is no definitive relation between $I(B_i; Z|B_0, \ldots, B_{i-1})$ and $I(B_i;Y)$. The mutual information $I(B_i;Z_i)$ in (28) is the constrained capacity of the channel $B_i \to Z_i$ shown in Figure 3(c). Equality in (28) is achieved if Z_i is a sufficient statistic for B_i given Z. Inequality (29) holds because $I^{\mathrm{gmi}}_{q_{B_i,Y}}$ is just an achievable rate by a mismatched decoding, whereas $I(B_i;Z_i)$ is the maximum achievable rate by matched decoding over the channel $B_i \to Z_i$.

Inequality (28) suggests that Z_j, $j \neq i$, can provide further information for the decoding of B_i. In between the two extremes of using only Z_i and using all m elements of Z, we might opt to process a subset $R_i = [Z_i, \{Z_j\}]$ of $1 < m_i < m$ elements of Z to produce decoding metrics for B_i. Partitioning $X \to Z$ into this type of binary-input reduced-dimensional output channel is similar to retaining only selected dependency links in reduced-layer MLC [18]. The resulting channel is included in Figure 3(d) and the inequalities

$$I(B_i; Z_i) \leq I(B_i; R_i) \leq I(B_i; Z) \tag{30}$$

hold for its associated mutual information. In summary, we obtain the following inequality chain:

$$I^{\text{gmi}}_{q_{X,Y}} \leq \sum_{i=0}^{m-1} I^{\text{gmi}}_{q_{B_i,Y}} \leq \sum_{i=0}^{m-1} I(B_i; Z_i) \leq \sum_{i=0}^{m-1} I(B_i; R_i) \leq \sum_{i=0}^{m-1} I(B_i; Z) \leq \begin{cases} \sum_{i=0}^{m-1} I(B_i; Y) \\ I(X; Z) \end{cases} \leq I(X; Y) \ . \tag{31}$$

2) Metric-Mismatch Correction: The processing of original LLRs to achieve the above rates can be considered as metric-mismatch correction. The matched bit-metrics for BICM transmission over the cascaded channel $X \to Z$ corresponds to corrected LLRs

$$\Lambda_{p_{Z|B_i}}(z) = \ln \frac{p_{Z|B_i}(z|0)}{p_{Z|B_i}(z|1)} \tag{32}$$

for $i = 0, \ldots, m-1$. This metric correction realizes the rate $I(B_i; Z)$ over the binary-input channel $B_i \to Z$, and, considering (31), it is the optimal correction in terms of achievable rate. The bit-metric correction corresponding to the channel $B_i \to R_i$ and achievable rate $I(B_i; R_i)$ is given by

$$\Lambda_{p_{R_i|B_i}}(r_i) = \ln \frac{p_{R_i|B_i}(r_i|0)}{p_{R_i|B_i}(r_i|1)} \ . \tag{33}$$

Finally, the scalar metric correction

$$\Lambda_{p_{Z_i|B_i}}(z_i) = \ln \frac{p_{Z_i|B_i}(z_i|0)}{p_{Z_i|B_i}(z_i|1)} \tag{34}$$

leads to $I(B_i; Z_i)$. Since metrics (32), (33), and (34) match to their corresponding binary-input channels, their binary I-curves are already aligned at $s = 1$. As a result, the BICM GMI with these metrics is equal to $\sum_{i=0}^{m-1} I(B_i; Z)$, $\sum_{i=0}^{m-1} I(B_i; R_i)$, and $\sum_{i=0}^{m-1} I(B_i; Z_i)$, respectively. While, according to (31), the associated BICM GMI degrades from (32) to (34), the computational complexity for metric correction is also reduced. This trade-off renders (33) and (34) potentially attractive.

The scalar LLR correction (34) has been studied in the literature [6], [19]–[22], cf. also [23]. In [6], (34) has been shown to be the optimum scalar metric correction in terms of GMI, a fact that is also clear from the above derivation. It has further been pointed out in [6] that non-scalar metric correction functions could further increase the GMI. We have provided such corrections in (32) and (33).

In practice, the correction functions are prepared offline and stored as look-up tables. Online evaluation is then done by table look-up and possibly with additional interpolation [22], [23]. For clarity, we summarize all bit-metric manipulations and their effects in the table below.

TABLE

BICM METRIC MANIPULATIONS AND THEIR EFFECTS.

Metric Manipulation	**Effect**
Original mismatched bit metrics $\Lambda_{q_{B_i,Y}}(y)$	$I^{\text{gmi}}_{q_{X,Y}} \leq \sum_{i=0}^{m-1} I^{\text{gmi}}_{q_{B_i,Y}}$ is achievable.
Scale all LLRs by the same factor $c = s_{q_{X,Y}}$: $\Lambda_{q'_{B_i,Y}}(y) = s_{q_{X,Y}} \Lambda_{q_{B_i,Y}}(y)$	Shift the critical point of the BICM I-curve to 1, aim to improve the performance of sum-product SBS decoding.
Scale LLRs differently by $c_i = s_{q_{B_i,Y}}/s^*$ for some $s^* > 0$: $\Lambda_{q'_{B_i,Y}}(y) = (s_{q_{B_i,Y}}/s^*)\Lambda_{q_{B_i,Y}}(y)$	Binary I-curves are aligned at s^*. $I^{\text{gmi}}_{q'_{X,Y}} = \sum_{i=0}^{m-1} I^{\text{gmi}}_{q_{B_i,Y}}$ is achievable. Choose $s^* = 1$ in sum-product decoding.
Apply scalar metric-mismatch correction: $\Lambda_{p_{Z_i\|B_i}}(z_i) = \ln \frac{p_{Z_i\|B_i}(z_i\|0)}{p_{Z_i\|B_i}(z_i\|1)}$	Bit metrics are matched to the cascaded channels $B_i \to Z_i$. BICM GMI is $\sum_{i=0}^{m-1} I(B_i;Z_i)$.
Apply reduced-dimensional vector metric-mismatch correction: $\Lambda_{p_{R_i\|B_i}}(r_i) = \ln \frac{p_{R_i\|B_i}(r_i\|0)}{p_{R_i\|B_i}(r_i\|1)}$	Bit metrics are matched to the cascaded channels $B_i \to R_i$, BICM GMI is $\sum_{i=0}^{m-1} I(B_i;R_i)$.
Apply optimal vector metric-mismatch correction: $\Lambda_{p_{Z\|B_i}}(z) = \ln \frac{p_{Z\|B_i}(z\|0)}{p_{Z\|B_i}(z\|1)}$	Bit metrics are matched to the cascaded channels $B_i \to Z$, BICM GMI is $\sum_{i=0}^{m-1} I(B_i;Z)$.

3) Remark: Inequality (31) also shows that no metric manipulation allows BICM to attain a GMI better than $\sum_{i=0}^{m-1} I(B_i;Y)$, i.e., the GMI of matched BICM over the original channel $X \to Y$. To achieve $I(X;Z)$ or $I(X;Y)$ with binary codes, we need to use MLC with multistage decoding [9] applied to the channels $X \to Z$ and $X \to Y$, respectively.

IV. APPLICATIONS

In this section, we present and discuss a number of illustrative and relevant examples for BICM transmission applying the metric manipulations described in the previous sections. We assume uniform input in all cases. The binary I-curves are obtained from (18) via Monte-Carlo integration.

A. Discrete Metrics and Metric Correction

1) Setup: Metric corrections are relatively easy to implement by means of look-up tables if the mismatched metrics are drawn from a small set of discrete values. Such cases arise if quantization and in particular hard detection is applied at the receiver. In the following, we consider the example of 8-ary amplitude-shift keying (8-ASK) transmission over the additive white Gaussian noise (AWGN) channel with hard detection. We apply binary reflected Gray labeling with $[b_0b_1b_2] = [000], [100], [110], [010], [011], [111], [101], [001]$ for the eight signal points from left to right. This is the best labeling in the moderate SNR range [24]. Let the SNR be equal to 6.43 dB, at which matched BICM attains a GMI of $I^{\mathrm{gmi}}_{q_{X,Y}} = \sum_{i=0}^{2} I(B_i;Y) = 1.50$ bpcu, and $I(X;Y) = 1.56$ bpcu. Hard detection that produces LLRs $+1$ and -1 leads to the GMI $I^{\mathrm{gmi}}_{q_{X,Y}} = 1.07$ bpcu, which is the maximum of the BICM I-curve $I_{q_{X,Y}}(s) = \sum_{i=0}^{2} I_{q_{B_i,Y}}(s)$, attained at $s_{q_{X,Y}} = 1.65$. The I-curves for matched and hard-decision decoding are plotted in Figure 4(d).

2) Metric-Mismatch Correction: We now examine the effect of metric manipulation. Consider level 2, whose I-curves are shown in Figure 4(c). With matched detection, the binary GMI is $I(B_2;Y) = 0.77$ bpcu. With hard detection, $B_2 \to Z_2$ is a BSC with the GMI equal to $I(B_2;Z_2) = 0.63$ bpcu, cf. Example 1. For a BSC, scalar correction (34) is identical to the scaling that shifts the critical point to 1 and leaves the GMI unchanged (line Z_2 in Figure 4(c)). On the other hand, the optimum vector correction (32) yields $I(B_2;Z) = 0.75$ bpcu (line $Z_2Z_0Z_1$ in Figure 4(c)), which is significantly higher than $I(B_2;Z_2)$ and rather close to $I(B_2;Y)$. The price for this is a more complex mapping. In scalar correction, we map z_2 from two input values $\{1,-1\}$ to two output values $\{2.56,-2.56\}$, i.e., $\Lambda_{p_{Z_2|B_2}}(1) = 2.56$ and $\Lambda_{p_{Z_2|B_2}}(-1) = -2.56$. In optimum vector correction, we need a larger look-up table to map $[z_2,z_0,z_1]$ from $\{[1,1,1],[1,-1,1],[1,-1,-1],[1,1,-1],[-1,1,-1],[-1,-1,-1],[-1,-1,1],[-1,1,1]\}$ to the corrected LLRs $\{12.5, 7.40, 3.63, 1.05, -1.05, -3.63, -7.40, -12.5\}$. Between these two correction methods, we have two choices for reduced-dimensional vector correction (33), namely

$R_2 = \{Z_2, Z_0\}$ or $R_2 = \{Z_2, Z_1\}$, each of which maps four input values to four output values. The two corresponding I-curves in Figure 4(c) are labeled Z_2Z_0 and Z_2Z_1, respectively. Since $I(B_2; Z_2Z_0) < I(B_2; Z_2Z_1)$, the latter is preferred.

We have a BAC at both level 0 and 1. For level 1, we can see from Figure 4(b) that scalar correction hardly increases the GMI. It is interesting to observe that correction with $R_1 = \{Z_1, Z_2\}$ yields the same I-curve as scalar correction, whereas correction with $R_1 = \{Z_1, Z_0\}$ yields the same I-curve as the optimum correction. For level 0, different correction functions result in identical binary I-curves, as shown in Figure 4(a). These phenomena can be explained from examining the labeling of signal points. Due to space limitation, we only explain why knowing z_0 helps to increase the GMI at level 1, whereas knowing z_2 does not. Consider the labeling bits at level 1. They are $\{0, 0, 1, 1, 1, 1, 0, 0\}$ for the eight symbols from left to right. We can divide the four labeling bits 1 into two groups: the outer two bits that are adjacent to a bit 0, and the other two inner bits which are not. To better approach the performance of the matched decoding, we should distinguish if a received bit 1 is an outer bit or an inner bit. Indeed, additional knowledge about z_0 tell us if the received bit 1 at level 1 is an outer bit (when $z_0 = -1$) or not (when $z_0 = 1$). On the other hand, knowing z_2 would not help. Similarly, the four labeling bits 0 can be divided into two groups, and knowledge of z_0, but not z_2, helps to distinguish if the received bit 0 is an inner or an outer bit.

The BICM I-curve for scalar and the best of all metric-mismatch corrections are included in Figure 4(d). For the latter, full vector correction is only required for level 2, while scalar correction and reduced-dimensional correction are sufficient at level 0 and level 1, respectively. The increase in the GMI by scalar correction comes mostly from the effect of having all the binary curves aligned at $s = 1$. Optimum correction results in a much improved GMI of 1.40 bpcu, which is 93% of the GMI for matched BICM.

3) Throughput: Using the Raptor code from Example 1, the simulated average throughput is shown in Figure 4(d) (markers without lines). We observe that the throughput closely follows the associated GMIs if metric-mismatch correction is applied. In these cases, the GMI is achieved at $s = 1$. In the case of hard detection metrics, the gap between GMI and simulated rate is significantly larger. This phenomenon has also been observed in Figure 2. It corroborates our discussion in Section III-B that, when $s_{q_{X,Y}} > 1$, the achieved throughput by sum-product SBS decoding seems to be determined by $I_{q_{X,Y}}(1)$ rather than the GMI.

B. Pulse-Position Modulation with Max-log Metric

Our next practical example considers M-ary pulse-position modulation (PPM) transmission for free-space optical communication, cf. e.g. [25]. Each M-ary PPM symbol is a vector $x = [x_0 \dots x_{M-1}]$ with exactly one element equal to 1 (*on* slot) and the others equal to 0 (*off* slots). Let $y = [y_0 \dots y_{M-1}]$ denote the corresponding received vector, and let us apply the popular photon-counting channel model [25]

$$y_i = x_i s_i + n_i \ , \tag{35}$$

where s_i and n_i are i.i.d. Poisson random variables with mean λ_s and λ_n, respectively. The channel transition probabilities are given by

$$p(y_i|x_i) = \frac{(\lambda_s x_i + \lambda_n)^{y_i}}{y_i!} \exp\left(-[\lambda_s x_i + \lambda_n]\right) \ , \tag{36}$$

and $p(y|x) = \prod_{i=0}^{M-1} p(y_i|x_i)$. Since all PPM symbols have exactly one element 1 and $M-1$ elements 0, it follows that

$$p(y|x) \propto \left(1 + \frac{\lambda_s}{\lambda_n}\right)^{y_o(x)} \ , \tag{37}$$

where $y_o(x)$ is the magnitude of the slot of y which corresponds to the *on* slot of x. The matched LLR for PPM is

$$\Lambda_{p_{Y|B_i}}(y) = \ln \sum_{x \in \mathcal{X}_i^0} \left(1 + \frac{\lambda_s}{\lambda_n}\right)^{y_o(x)} - \ln \sum_{x \in \mathcal{X}_i^1} \left(1 + \frac{\lambda_s}{\lambda_n}\right)^{y_o(x)} \ . \tag{38}$$

The simplified max-log metric is

$$\Lambda_{q_{B_i,Y}}(y) = \left(\max_{x \in \mathcal{X}_i^0} y_o(x) - \max_{x \in \mathcal{X}_i^1} y_o(x)\right) \ln\left(1 + \frac{\lambda_s}{\lambda_b}\right) \ , \tag{39}$$

which has considerably lower computational complexity than (38).

A special property of PPM is that (i) all symbol labelings are equivalent and (ii) all binary levels have identical I-curves if the same binary metrics are used. This results from the orthogonality of PPM constellations, which means that labelings can be transformed from one to another by a permutation of time slots. Therefore, regardless of the labeling, the BICM GMI is given by $I^{\text{gmi}}_{q_{X,Y}} = \sum_{i=0}^{m-1} I^{\text{gmi}}_{q_{B_i,Y}} = m I^{\text{gmi}}_{q_{B_j,Y}}$ for any metric $q_{B_i,Y}(b,y)$ (e.g., matched and max-log metric given above) and level $j \in \{0, \dots, m-1\}$, $m = \log(M)$.

Figure 5 shows the GMI of matched metric (38) and max-log metric (39) as function of the SNR defined as $\lambda_s/(M\lambda_n)$ for the example of 64-PPM and $\lambda_n = 0.2$ [26]. We observe only a

relatively small gap between the two GMIs. This suggests that the simpler mismatched metric (39) could be applied with little loss in achievable rate. Also included in Figure 5 is $I_{q_{X,Y}}(1)$ for the max-log metric, for which a notable gap to the corresponding mismatched GMI can be seen, especially for low SNR. Following the discussion in Section III-B, we expect that scaling of the max-log LLR such that the critical point is shifted to 1 should be applied to improve the performance of sum-product decoding. This prediction is confirmed by the results presented in Figure 6 for an example SNR of -8 dB. It shows the I-curves for matched, max-log, and scaled max-log metric with the scaling factor $c = s_{q_{X,Y}} = 0.56$, together with simulated throughputs for sum-product and max-product decoding. The throughput figures are obtained from simulation using the same Raptor code as in Example 1. We observe that the simulated throughput using sum-product decoding well approaches the associated GMI for matched metric. For the max-log metric, however, the gap between throughput and GMI is significantly larger. With scaling, the throughput accomplished with sum-product decoding is significantly improved to 1.96 bpcu compared to 1.74 bpcu without scaling. More specifically, the gap between throughput and GMI is closed by 60%. Finally, the performance of max-product decoding is notably inferior to sum-product decoding and, as expected, is not changed by scaling.

C. MIMO-QAM with Max-Log Metric and LLR Clipping

The third and final illustration of BICM with mismatched decoding and metric-mismatch correction uses the example considered in [6, Sec. IV]. The transmission system is a 2×2 multiple-input multiple-output (MIMO) system with 16-ary quadrature amplitude modulation (16-QAM) and Rayleigh fading channels, and the average SNR is fixed to 9.13 dB. Furthermore, the BICM demodulator uses the max-log metric and the max-log LLR is clipped to the range $[-2, +2]$. LLR clipping is helpful to reduce complexity in list-based detection [22]. It has been shown in [6, Sec. IV] that the optimum scalar correction (34) improves the GMI and the bit-error rate (BER) performance of the coded scheme. In this section, we also consider LLR scaling and a hybrid scalar correction as explained below.

We assume a binary reflected Gray labeling for the 16-QAM symbols. The 2×2 MIMO system with 16-QAM has in total $m = 8$ binary levels, of which four are equivalent to level 0 and four to level 1. Hence, we only need to consider those two levels when showing results. Figure 7(a) presents the I-curves of the levels with matched and clipped max-log metrics. The

curves for the matched metrics serve as an upper bound and will be used to gauge the success of mismatched-metric manipulation. It can be seen that the two binary I-curves for the clipped max-log metric are misaligned. We expect that scaling to align them at $s^* = 1$ will increase the BICM GMI and improve sum-product decoding performance. The BICM GMI curves for matched, clipped max-log, and scaled clipped max-log metric are shown in Figure 7(b). Also included are simulated throughputs, again using the Raptor code from Example 1 with sum-product decoding. We observe that, for clipped max-log with $s_{q_{X,Y}} = 1.50 > 1$, the achievable throughput seems to be upper bounded by $I_{q_{X,Y}}(1)$. This might explain the large gap between the BER curve and the GMI limit of the uncorrected LLR in [6, Fig. 2(b)]. Metric scaling aligns the binary I-curves at $s^* = 1$ and leads to an improved GMI. While the GMI increase is only slightly, the throughput improvement is much more significant.

Applying the optimum scalar metric-mismatch correction (34), also considered in [6, Sec. IV], [22, Sec. V], further improves both GMI and the performance with sum-product decoding. At the same time, it is more complex than scaling as the correction requires table look-up and interpolation (see also the plot of the scalar correction function in Figure 8 and the discussion below). Noting that metric scaling treats all values $\Lambda_{q_{B_i,Y}}(y)$ the same, even though the two extreme values -2 and $+2$ would warrant a special consideration, we propose the following hybrid metric manipulation for this particular case:

$$\Lambda_{q'_{B_i,Y}}(y) = \begin{cases} \ln \frac{p_{Z_i|B_i}(z_i|0)}{p_{Z_i|B_i}(z_i|1)} \,, & \text{if } z_i = \pm 2 \\ c_i z_i \,, & \text{otherwise} \,. \end{cases} \tag{40}$$

That is, the two extreme values are mapped as in the optimum scalar correction, and the immediate values are scaled with a factor such that the resulting I-curve peaks at $s = 1$. This correction function is indeed a good approximation of the optimum scalar correction for the symmetric channel at level 1. However, this is not the case for the asymmetric channel at level 0. Hence, we apply channel symmetrization according to [13] as discussed in Example 1 before using the hybrid rule (40). The different metric manipulations are plotted in Figure 8. From Figure 7, we observe that hybrid manipulation results in I-curves and throughput performances that are practically identical to those achieved with optimum scalar correction. Considering its simpler implementation, this hybrid metric manipulation would be the method of choice for this application example.

V. Conclusion

In this paper, we studied BICM with mismatched decoding metrics. Following recent works, we adopted the GMI as a pertinent performance measure. We showed that scaling of logarithmic bit-metrics can improve the BICM GMI. We also suggested and provided numerical evidence that metric scaling also improves throughput in practical coding schemes using SBS decoding, even if the GMI remains unchanged. Furthermore, we studied general mismatched metric correction methods, including a previously proposed scalar correction. We presented a number of practically relevant applications in which mismatched demodulation occurs, and our numerical results highlighted the benefits and performance-complexity trade-offs for the different mismatch-metric correction approaches.

References

[1] E. Zehavi, "8–PSK trellis codes for a rayleigh channel," *IEEE Trans. Commun.*, vol. 40, no. 5, pp. 873–884, May 1992.

[2] A. Guillén i Fàbregas, A. Martinez, and G. Caire, "Bit-interleaved coded modulation," *Found. Trends Commun. Inf. Theory*, vol. 5, no. 1-2, pp. 1–135, 2008.

[3] A. Martinez, A. Guillén i Fàbregas, G. Caire, and F. Willems, "Bit-interleaved coded modulation revisited: A mismatched decoding perspective," *IEEE Trans. Inf. Theory*, vol. 55, no. 6, Jun. 2009.

[4] G. Kaplan and S. Shamai, "Information rates and error exponents of compound channels with application to antipodal signaling in a fading environment," *Archiv für Elektronik und Übertragungstechnik (AEÜ)*, vol. 47, no. 4, pp. 228–239, 1993.

[5] N. Merhav, A. Lapidoth, and S. Shamai, "On information rates for mismatched decoders," *IEEE Trans. Inf. Theory*, vol. 40, no. 6, pp. 1953–1967, 1994.

[6] J. Jaldén, P. Fertl, and G. Matz, "On the generalized mutual information of BICM systems with approximate demodulation," in *IEEE Inf. Theory Workshop*, Cairo, Egypt, Jan. 2010.

[7] R. Gallager, *Information Theory and Reliable Communication*. New York: Wiley, 1968.

[8] G. Caire, G. Taricco, and E. Biglieri, "Bit-interleaved coded modulation," *IEEE Trans. Inf. Theory*, vol. 44, pp. 927–946, May 1998.

[9] U. Wachsmann, R. Fischer, and J. B. Huber, "Multilevel codes: theoretical concepts and practical design rules," *IEEE Trans. Inf. Theory*, vol. 45, no. 5, pp. 1367–1391, Jul. 1999.

[10] F. Kschischang, B. Frey, and H. Loeliger, "Factor graphs and the sum-product algorithm," *IEEE Trans. Inf. Theory*, vol. 47, no. 2, pp. 498–519, 2001.

[11] A. Shokrollahi, "Raptor codes," *IEEE Trans. Inf. Theory*, vol. 52, no. 6, pp. 2551–2567, Jun. 2006.

[12] X.-Y. Hu, E. Eleftheriou, and D. Arnold, "Regular and irregular progressive edge-growth Tanner graphs," *IEEE Trans. Inf. Theory*, vol. 51, no. 1, pp. 386–398, Jan. 2005.

[13] J. Hou, P. Siegel, L. Milstein, and H. Pfister, "Capacity-approaching bandwidth-efficient coded modulation schemes based on low-density parity-check codes," *IEEE Trans. Inf. Theory*, vol. 49, no. 9, pp. 2141–2155, 2003.

[14] H. Saeedi and A. H. Banihashemi, “Performance of belief propagation for decoding LDPC codes in the presence of channel estimation error,” *IEEE Trans. Commun.*, vol. 55, no. 1, pp. 83 –89, Jan. 2007.

[15] J. Chen, A. Dholakia, E. Eleftheriou, M. Fossorier, and X.-Y. Hu, “Reduced-complexity decoding of LDPC codes,” *IEEE Trans. Commun.*, vol. 53, no. 8, pp. 1288–1299, 2005.

[16] G. Lechner, “Efficient Decoding Techniques for LDPC Codes,” Ph.D. dissertation, Vienna Univ. of Tech., Jul. 2007.

[17] S. Papaharalabos and P. Mathiopoulos, “Simplified sum-product algorithm for decoding LDPC codes with optimal performance,” *IEE Electronics Letters*, vol. 45, no. 2, pp. 116–117, 2009.

[18] T. T. Nguyen and L. Lampe, “Rateless multilevel coding and applications,” in *Proc. IEEE Global Telecommun. Conf. (GLOBECOM)*, Nov. 2009, pp. 1 –7.

[19] A. Burg, M. Wenk, and W. Fichtner, “VLSI implementation of pipelined sphere decoding with early termination,” in *Proc. Europ. Sig. Processing Conf.*, Florence, Italy, Sep. 2006.

[20] S. Schwandter, P. Fertl, C. Novak, and G. Matz, “Log-likelihood ratio clipping in MIMO-BICM systems: Information geometric analysis and impact on system capacity,” in *Proc. IEEE ICASSP*, Taipei, Taiwan, Apr. 2009, pp. 2433–2436.

[21] C. Novak, P. Fertl, and G. Matz, “Quantization for soft-output demodulators in bit-interleaved coded modulation systems,” in *Proc. IEEE Intl. Symp. Inf. Theory (ISIT)*, Seoul, Korea, Jun. 2009, pp. 1070–1074.

[22] C. Studer and H. Bölcskei, “Soft-input soft-output single tree-search sphere decoding,” *IEEE Trans. Inf. Theory*, initial submission June 2009, revised Apr. 2010, accepted May 2010. [Online]. Available: http://www.nari.ee.ethz.ch/commth/pubs/p/sisosts09

[23] M. van Dijk, A. J. E. M. Janssen, and A. G. C. Koppelaar, “Correcting systematic mismatches in computed log-likelihood ratios,” *Europ. Trans. Telecommun.*, vol. 14, no. 3, pp. 227–244, 2003.

[24] C. Stierstorfer and R. F. H. Fischer, “(Gray) mappings for bit-interleaved coded modulation,” in *Proc. IEEE Vehicular Tech. Conf. (VTC) Spring*, May 2007, pp. 1703 –1707.

[25] S. J. Dolinar, J. Hamkins, B. E. Moision, and V. A. Vilnrotter, “Optical modulation and coding,” in *Deep Space Optical Communications*, H. Hemmati, Ed. Wiley-Interscience, Apr. 2006.

[26] J. Hamkins and B. Moision, “Multipulse pulse-position modulation on discrete memoryless channels,” *JPL Interplanetary Network Progress Report*, vol. 42, p. 161, May 2005.

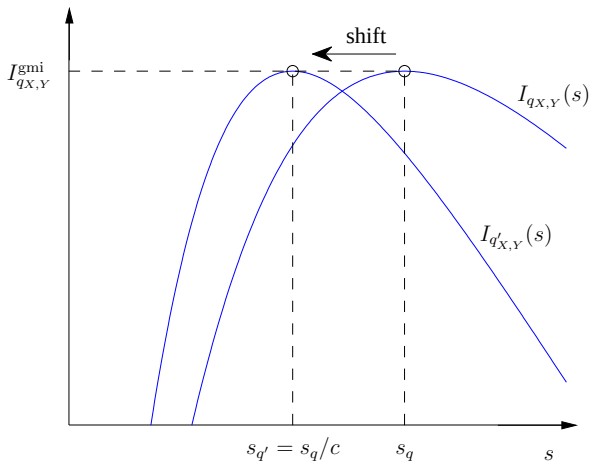

Fig. 1. Illustration of the horizontal shift of the peak of the I-curve when using metric $q'_{X,Y}(x,y) = [q_{X,Y}(x,y)]^c$.

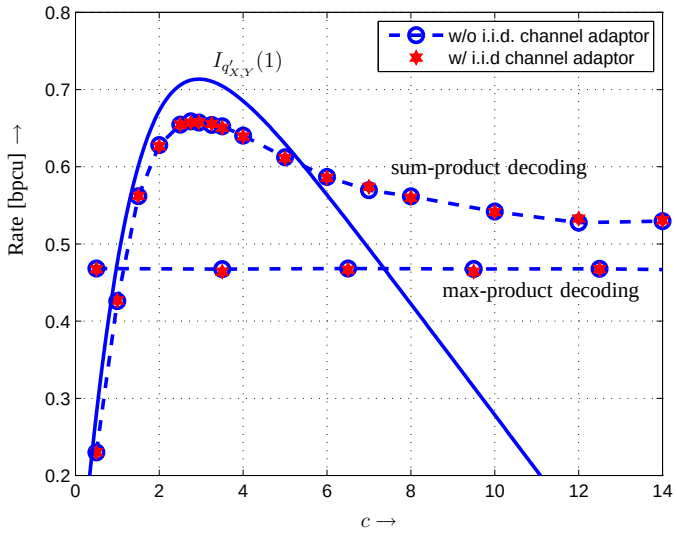

Fig. 2. Throughput achieved with a Raptor code over a BAC and SBS decoding with mismatched metrics versus the metric-scaling parameter c (see Example 1 for details).

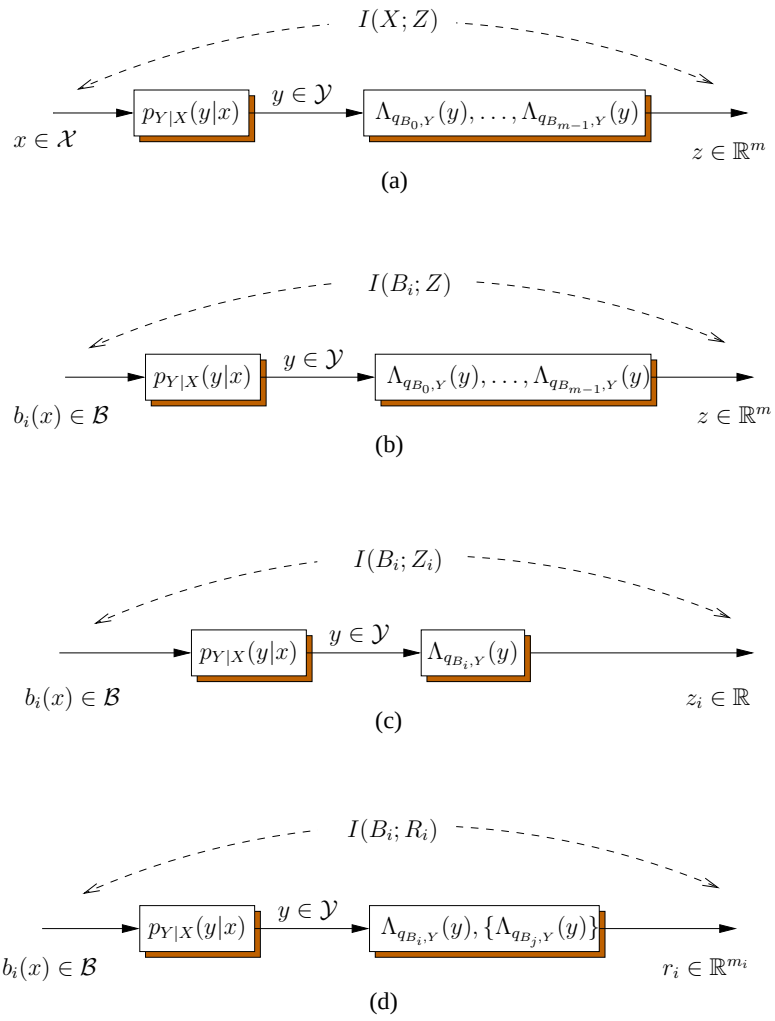

Fig. 3. BICM demodulator as part of a cascaded channel. Also indicated above each block diagram is the associated average mutual information. (a) symbol-input cascaded channel; (b), (c) and (d) different binary-input cascaded channels.

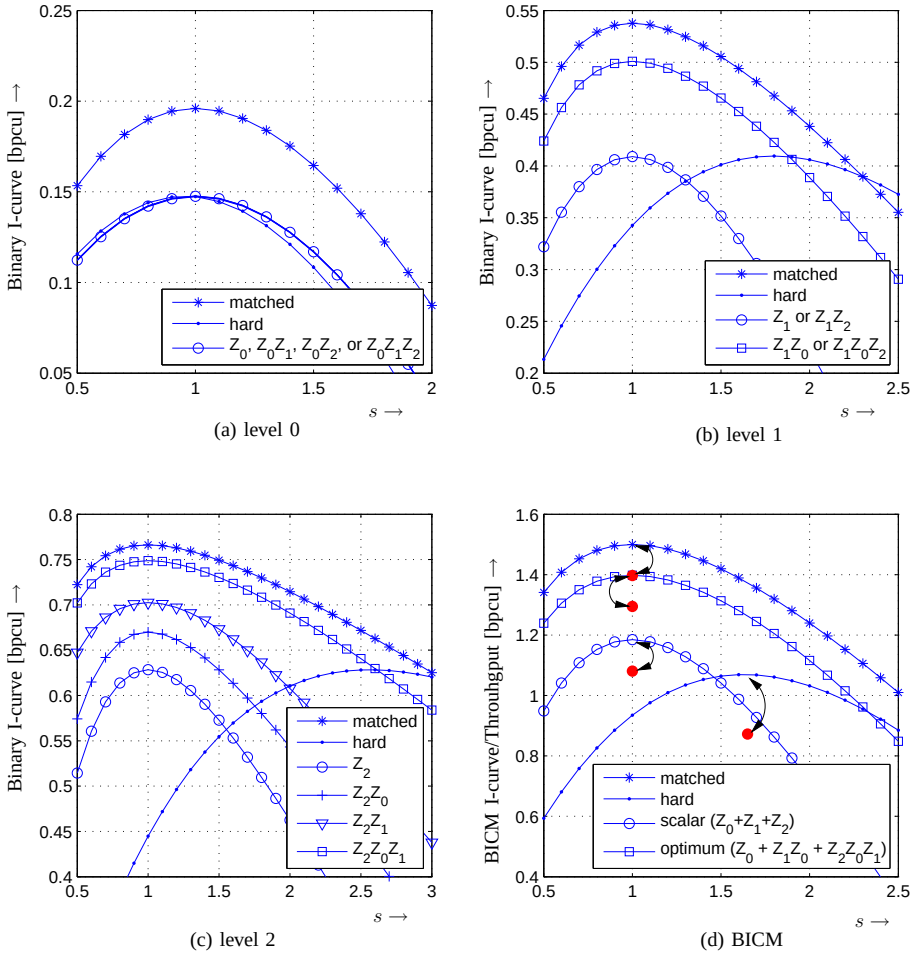

(a) level 0 (b) level 1

(c) level 2 (d) BICM

Fig. 4. I-curves for 8-ASK transmission over the AWGN channel with matched detection ('matched'), hard detection ('hard'), and different metric-mismatch corrections (identified by the used LLRs z_i in the subfigures). Subfigures (a)-(c) show I-curves for binary levels. Subfigure (d) shows BICM I-curves. The bullet markers show simulated throughput using a Raptor code and sum-product decoding, and the double-arrowed arcs link the simulated points to the peak of the corresponding I-curves.

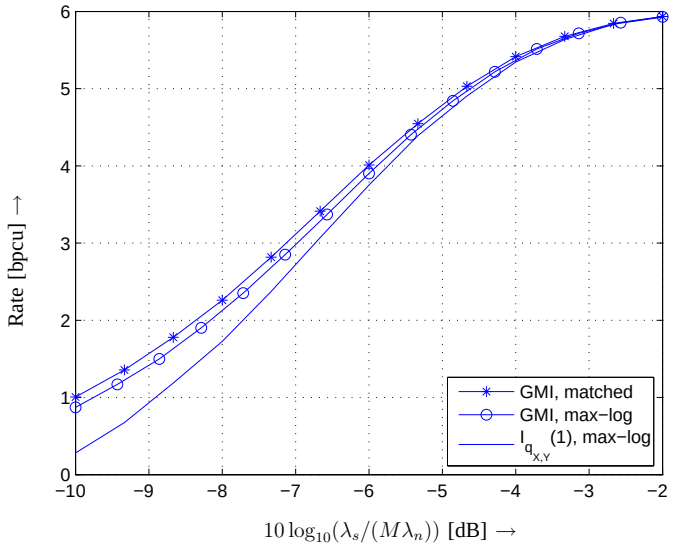

Fig. 5. BICM GMI for decoding with matched metric and max-log metric, and $I_{q_{X,Y}}(1)$ for max-log metric. 64-PPM transmission over Poisson channel. Background radiation has mean $\lambda_n = 0.2$ photon/slot.

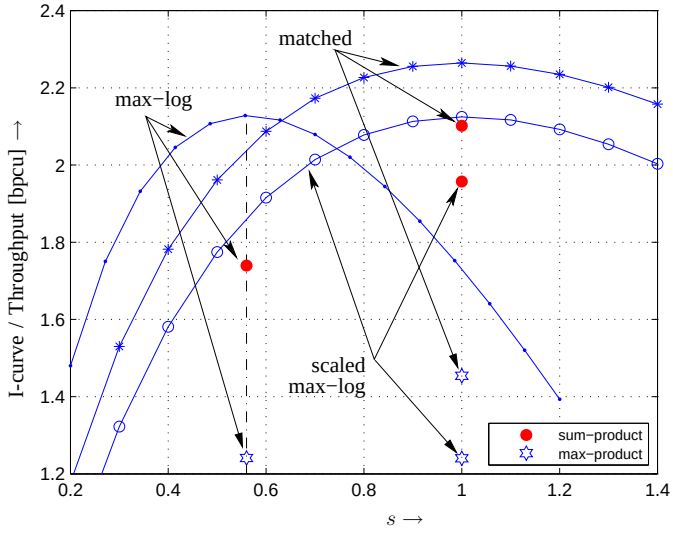

Fig. 6. BICM I-curve and simulated rates. Matched, max-log, and scaled max-log metric with the scaling factor $c = s_{q_{X,Y}} = 0.56$. The bullet markers show simulated rates using a Raptor code and sum-product and max-product decoding. 64-PPM over Poisson channel at SNR of $10\log_{10}(\lambda_s/(M\lambda_n)) = -8$ dB and $\lambda_n = 0.2$ photon/slot.

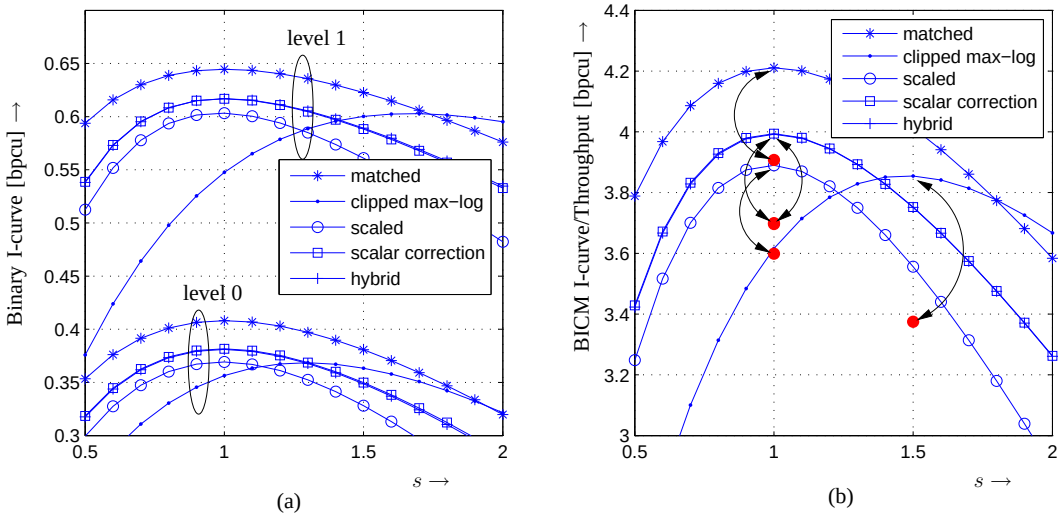

Fig. 7. I-curves for 2×2 MIMO transmission with 16-QAM over Rayleigh fading at an SNR of 9.13 dB (as in [6, Sec. IV]). Matched, clipped max-log, scaled clipped max-log metric which shifts the critical point of the I-curve to 1, scalar metric-mismatch correction, and a hybrid correction. (a) I-curves for binary levels. (b) BICM I-curves. The bullet markers show simulated rates using a Raptor code and sum-product decoding, and the double-arrowed arcs link the simulated points to the peak of the corresponding I-curves. Note that the curves for 'scalar correction' and 'hybrid' are numerically on top of each other.

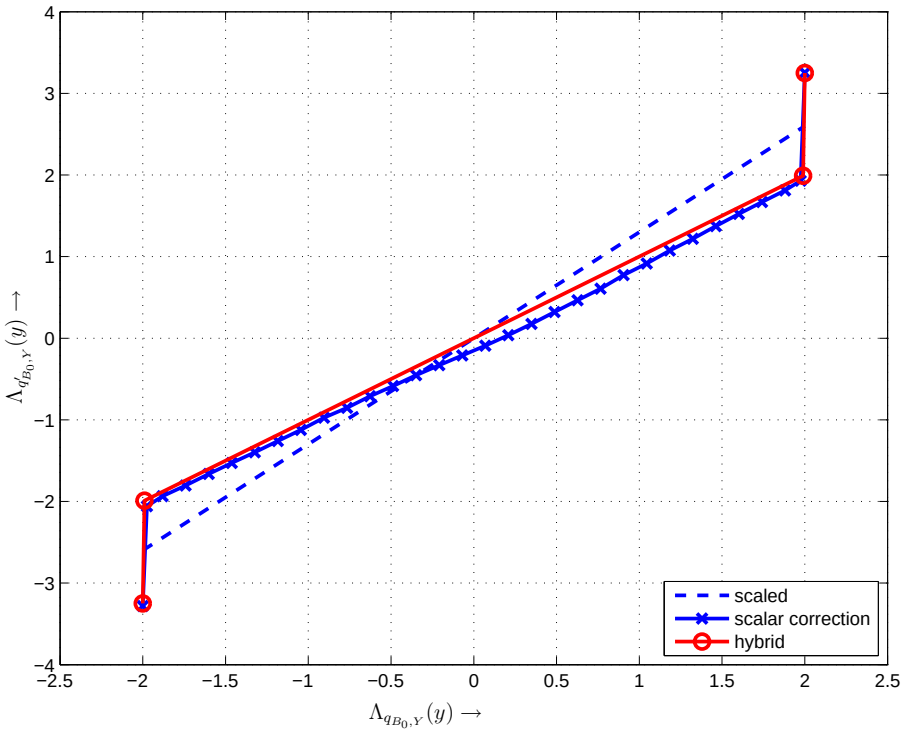

Fig. 8. Different metric manipulations for binary level 0 of 2×2 MIMO transmission with 16-QAM Rayleigh fading and SNR of 9.13 dB. Hybrid metric manipulation requires channel symmetrization before applying (40).